

Upper mantle seismic anisotropy beneath Antarctica and the Scotia Sea region

Christian Müller

Alfred Wegener Institute for Polar and Marine Research, Postfach 120161, D-27515 Bremerhaven, Germany. E-mail: cmueller@awi-bremerhaven.de

Accepted 2001 May 20. Received 2001 May 10; in original form 2000 August 8

SUMMARY

Recent investigations on shear wave splitting from recordings of permanent and temporary Antarctic seismological stations have led to a greater understanding of the upper mantle dynamics of the Scotia Sea region and the continental margin in the eastern Weddell Sea in terms of their tectonic evolution. The analysis of shear wave splitting from teleseismic core (*SKS*, *SKKS*, *PKS*) and direct *S* waves reveals the seismic anisotropy and the strain field of the upper mantle. Similar to the Caribbean, anisotropy structures in the Antarctic Peninsula and Scotia Sea regions are assumed to be influenced by mantle flows in easterly directions around the subducting Nazca plate. In general, anisotropy polarization directions in the Scotia Sea do not contradict this hypothesis, with polarizations oriented nearly E-W and therefore aligning with the suggested mantle flow patterns. Anisotropy strengths decrease from delay times of $\delta t = 1.8$ s (PMSA, Palmer Station) in the west towards the east with delay times of $\delta t = 0.3$ s beneath HOPE (South Georgia) and CAND (Candlemas, South Sandwich Islands). Nevertheless, a lithospheric and therefore fossil origin cannot be ruled out. Only the exceptionally high delay times at PMSA probably originate in part from recent asthenospheric flow around the subduction slab of the former Phoenix Plate beneath the northwestern margin of the Antarctic Peninsula. The continental margin of western Dronning Maud and Coats Land plays a crucial role in understanding the early processes during the break-up of Gondwana. Upper mantle seismic anisotropy with delay times well over $\delta t = 1$ s in this region gives new constraints on ancient deformation processes during break-up and former episodes. Two-layer modelling reveals Archaean anisotropy in the upper layer corresponding well to polarization directions of the South African Kaapvaal Craton. Lower layer anisotropy is assumed to have been created during early Gondwana rifting stages.

Key words: Antarctica, asthenospheric mantle flow, Gondwana break-up, lithospheric deformation, seismic anisotropy, shear wave splitting.

1 INTRODUCTION

In recent years, the analysis of seismic anisotropy has developed into a powerful tool for mapping deformations in the Earth's upper mantle. Investigations of seismic anisotropy allow the explanation of geodynamic processes that influence global plate movements. Upper mantle seismic anisotropy is mainly produced by lattice preferred orientation of highly anisotropic mantle peridotites during deformation processes (Nicolas & Christensen 1987; Ben Ismail & Mainprice 1998; Mainprice *et al.* 2000). Shear wave splitting is induced when a shear wave passes through an anisotropic medium. A formerly linear polarized shear wave is split into two orthogonal polarized waves that travel with different velocities. The splitting is characterized by the direction of fast wave polarization (ϕ) and

the time delay between split waves (δt). The time lag δt depends on the effective travel path of the waves and the intrinsic anisotropy of the medium. The orientation of the fast wave (ϕ) is related to the structural direction and in general parallels the deformation direction (Mainprice & Silver 1993). Therefore, a direct correlation exists between *S*-wave splitting, seismic anisotropy, geodynamic processes in the upper mantle and global tectonic evolution. Delay times (δt) are in the range 0–2 s, and the global average in continental mantle is 1.0 s (Silver 1996). The intrinsic *S*-wave anisotropy ranges from 2 to 5 per cent and, for the delay times mentioned above, corresponds to a thickness of the anisotropic layer of 100–300 km for a near-vertical ray path (Mainprice & Silver 1993; Ben Ismail & Mainprice 1998). In general, the fast polarization direction parallels the *a*-axis orientation of olivine, is oriented subparallel

to horizontal flow directions or strain directions in the upper mantle, and corresponds to fossil or recent deformation events or a combination of both. The origin of seismic anisotropy may be frozen-in structures from ancient tectonic episodes or ongoing deformation events or a combination of both. The question regarding the regions of origin of seismic anisotropy in the upper mantle (lithosphere: fossil anisotropy corresponding to ancient mountain-building events; or asthenosphere: recent, absolute or relative plate motions) is still a source of controversy (Silver 1996; Vinnik *et al.* 1992). Regions that were deformed at temperatures >900 °C and cooled below this threshold conserve the ‘frozen’ anisotropy information of this ancient tectonic episode. Shallow regions of seismic anisotropy that originate from recent deformation only occur in hot regions such as active rifts (Vauchez *et al.* 2000). In cold regions, anisotropy reflects information from past deformation. In these regions, recent deformation may produce anisotropic structures at depths greater than 200 km, which corresponds to $\delta t > 1\text{--}1.5$ s (Savage 1999). Collisional events such as mountain-building episodes in general produce strong transcurrent deformation subparallel to the strike of the mountain range. Fast polarization directions therefore parallel structural features and are explained by vertical coherent deformation of the underlying mantle (Silver 1996). In summary, seismic anisotropy is generated

by stress- and strain-induced deformation of lithosphere with frozen anisotropic structures from past tectonic episodes, recent asthenospheric plate motion, or similarly small-scale convection, or flow around barriers.

Until now, only a few studies have been conducted on shear wave splitting in Antarctica and surrounding regions. As the density of seismograph stations in Antarctica is very low, no systematically spatial investigation of upper mantle anisotropy is possible. Nevertheless, some of the existing permanent stations were used for shear wave splitting analysis (Barruol & Hoffmann 1999; Kubo *et al.* 1995; Pondrelli & Azzara 1998). In this contribution, recordings of temporary seismic stations supplemented by the German geodetic SCAR (Scientific Committee on Antarctic Research) GPS campaign (Dietrich 2000), BELO (Belgrano II), CAND (Candlemas Island), JUBY (Jubany Station), ROTH (Rothera Station), SIGY (Signy Station), the permanent GSN stations DRV (Dumont d’Urville Station), EFI (East Falkland Islands), HOPE (South Georgia), PMSA (Palmer Station) and SPA (South Pole Station), and the Alfred Wegener Institute stations VNA2 (Neumayer Station/Halvfær Ryggen), VNA3 (Neumayer Station/Søråsen) and SNAA (Sanae IV station) were analysed for shear wave splitting (Fig. 1 and Table 1). The aim of this study is to deduce anisotropy parameters beneath these Antarctic and sub-Antarctic

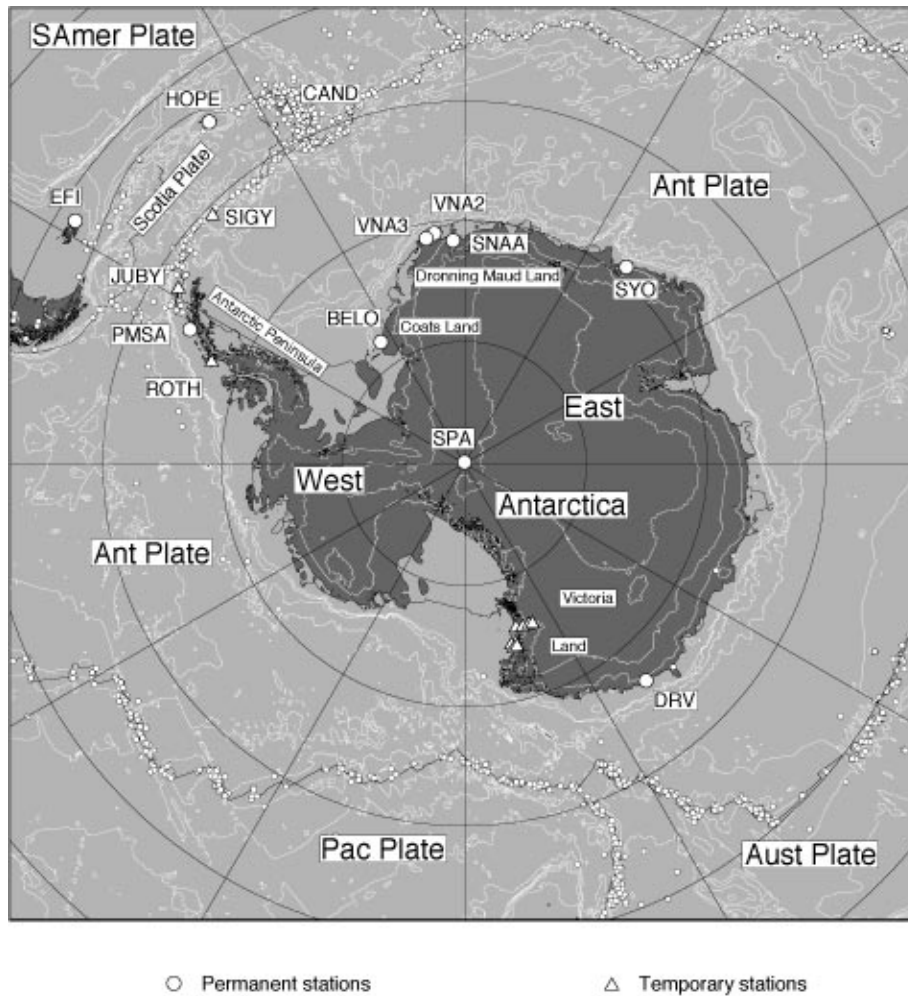


Figure 1. Antarctic and Subantarctic seismological stations used in this study. Small circles show earthquake epicentres according to the International Seismological Centre earthquake catalogue. Also shown are 1000 m topographic contours. Abbreviations are as follows: Ant Plate—Antarctic Plate; Aust Plate—Australian Plate; Pac—Pacific Plate; SAMer Plate—South American Plate.

Table 1. Station coordinates and averaged splitting parameters. In the case of two-layer modelling, the parameters of both layers are given. *KS denotes the use of core phases (*SKS*, *SKKS*, *PKS*).

Station	Lat.	Long.	Elev.	Location	ϕ (°)	δt (s)	Phases	Comments	
BELO	77.867°S	34.567°W	100 m	Belgrano II Station (ARG)	75	0.60	21 *KS, 7 S	AWI ¹ /IAA ² lower layer	
					90	0.8			upper layer
					50	0.8			AWI/BAS ³ — temporary
CAND	57.088°S	26.714°W	5 m	Candlemas Island, South Sandwich Islands	76	0.4	6 local S	temporary GEOSCOPE ⁴	
DRV	66.665°S	140.010°E	40 m	Dumont d'Urville Station (F)	100	0.92	4 *KS	IRIS ⁵ –GSN ⁶ lower layer	
EFI	51.680°S	58.060°W	110 m	Mount Kent, East Falklands Is. (GB)	88	1.10	12 *KS, 1 S	upper layer	
					35	0.8			
					85	0.8			
HOPE	54.284°S	36.488°W	20 m	Hope Point, South Georgia Island (GB)	73	0.28	7 *KS	IRIS–GSN	
JUBY	62.233°S	58.633°W	20 m	Jubany Station, South Shetland Islands (ARG)	110	1.26	1 *KS, 1 S	AWI/IAA— temporary	
PMSA	64.775°S	64.048°W	10 m	Palmer Station, Adelaide Island (USA)	86	1.82	14 *KS, 10 S, 3 ScS	IRIS–GSN lower layer	
					80	1.0			upper layer
					100	1.2			
ROTH	67.523°S	68.193°W	150 m	Rothera Station, Adelaide Island (GB)	118	1.35	1 *KS	AWI/BAS— temporary	
SIGY	60.717°S	45.600°W	30 m	Signy Station, South Orkney Islands (GB)	82	1.01	1 *KS, 1 S	AWI/BAS— temporary	
SNAA	71.671°S	2.838°W	850 m	Sanae IV Station, Vesleskarvet (RSA)	72	1.24	14 *KS, 2 S	AWI/CGS ⁷ lower layer	
					120	0.3			
					70	0.8			upper layer
SPA	89.982°S	0.000°E	2930 m	South Pole Station (USA)	68	1.28	2 *KS	IRIS–GSN	
VNA2	70.925°S	7.393°W	350 m	Neumayer Station, Halvfår Ryggen (GER)	64	1.16	28 *KS, 5 S, 4 ScS	AWI lower layer	
					110	0.5			
					60	1.0			upper layer
VNA3	71.243°S	9.670°W	480 m	Neumayer Station, Søråsen (GER)	64	1.18	28 *KS, 5 S, 3 ScS	AWI lower layer	
					90	0.4			
					60	0.8			upper layer

¹ Alfred-Wegener-Institut für Polar- und Meeresforschung, Bremerhaven² Instituto Antártico Argentino, Buenos Aires³ British Antarctic Survey, Cambridge⁴ Programme GEOSCOPE, Institut de Physique du Globe de Paris⁵ Incorporated Research Institutions for Seismology, Data Management Center, Seattle⁶ Global Seismograph Network⁷ Council for Geoscience, Pretoria

stations and discuss the results in the light of tectonic evolution and neotectonic processes of the Antarctic continent. The results will be discussed regarding possible relationships to frozen-in lithospheric origin, present-day asthenospheric mantle flow or a combination of both as two distinct anisotropic layers.

2 SHEAR WAVE SPLITTING MEASUREMENTS

Since the beginning of the 1990s the method of investigating teleseismic shear wave splitting has been developed into a standard tool of seismological analysis. Analysis of shear wave splitting reveals the anisotropy parameters in the upper mantle beneath the recording station (Silver & Chan 1991; Vinnik *et al.* 1989). Core phases such as *SKS*, *SKKS* and *PKS* are preferentially used since they pass through the liquid outer core as *P* waves and therefore lack any source-side anisotropic contribution. Another advantage of using core phases is the nearly vertical travel path through the upper mantle as well as the knowledge of the initial, linear polarization direction corres-

ponding to the backazimuth of the ray at the recording station. For a better azimuthal coverage some direct *S* waves were used as well. These were carefully chosen and only deep earthquakes were used to avoid contamination by source-side effects. In the case of splitting analysis for station CAND (Candlemas Island) no teleseismic events of sufficient quality could be used, but during the field campaign six deep events were recorded from the downgoing slab of the South Sandwich subduction zone. Fortunately, these events were nearly beneath the recording station. Also, the direct *S* waves of these events could be used for the examination of anisotropic structures between the hypocentre and the station.

For the inversion of anisotropy parameters the methods of (Silver & Chan 1991) were used. These two methods estimate the splitting parameters ϕ (fast polarization direction) and δt (delay time between split waves) assuming a single layer of hexagonal symmetry with a horizontal symmetry axis (Silver & Chan 1991). In this simple case, no backazimuthal variations in the splitting parameters occur. Nevertheless, these methods are applicable to any kind of anisotropy as long as the ray arrives

close to the vertical (Savage 1999). Splitting parameters were determined by particle motion analysis of each phase by means of a net grid search method by calculating the covariance matrix of the horizontal seismogram components and minimizing the corresponding eigenvalue for possible values of ϕ and δt . The splitting parameters are those values of $(\phi, \delta t)$ that provide the most singular covariance matrix, that is, that minimize the corresponding eigenvalue, and therefore reveal the most linear particle motion. Core phases travelling through an isotropic medium should have no energy on the transverse component. Using these phases, the initial polarization direction is equaled by the backazimuth, and splitting parameters are determined by minimizing the energy of the transverse component again by the net grid search technique. This second method was used to verify the results of the covariance method and to exclude other sources such as the origin of non-linear particle motion, for example, dipping layers or other large-scale lateral heterogeneities. The phases were carefully evaluated and those with a sufficient signal-to-noise ratio, clearly separated from other phases, were chosen and bandpass filtered individually in the frequency range between 0.05 and 0.5 Hz. The upper limit for low-pass filtering was 0.2 Hz to guarantee high resolution of the delay times for a typical value around 1 s. The following were used as diagnostics for successful splitting parameter estimations: (1) the seismograms corrected for anisotropy effects were examined with respect to linear particle motion, (2) successful removal of transverse energy in the case of core phases, and (3) comparable results for both methods of covariance analysis and minimizing transverse component energy. Some 'null' measurements were also found. In the case of null splitting no seismic anisotropy is present, or the initial polarization corresponds to either the fast or the slow polarization direction. In the latter cases, no δt estimation is possible but the ϕ direction should correspond to the initial polarization or be perpendicular to it. The study of azimuthal variations of splitting parameters yields better depth resolution of anisotropy. Therefore, the initial polarization directions must be known. In the case of core phases these are known from the backazimuths and in the case of direct S waves they are estimated from the polarization direction of linearized seismograms. As an example, Fig. 2 shows the analysis of an SKS wave recorded at station VNA3 and Fig. 3 shows an example of a null measurement found at station BELO.

The events used were selected from the Preliminary Determinations of Epicenters data catalogue of the US Geological Survey and phase arrival times were estimated using the IASPEI91 earth model (Kennett 1995). In general, data were chosen from earthquakes with magnitudes $m_b > 6.0$ and a distance range $85^\circ < \Delta < 120^\circ$ for the most prominent SKS waves. In a few cases phases of weaker events could also be used. For better azimuthal coverage PKS , $SKKS$ and deep-focus S and ScS were also used. In Table 1 the phases used are summarized. Direct S waves were used with hypocentres deeper than 200 km to avoid source-side contamination effects. Also, to avoid free-surface polarization effects only S waves with a steeper incident angle than the critical angle of 35° (Nuttli 1961) were chosen.

Fig. 4 shows the results of all events investigated for shear wave splitting. The number of analysed recordings varies strongly with the duration of operation of each station, their geographical location with respect to the main seismogenic region, and the noise conditions at the stations. Recordings from island stations such as CAND, EFI, HOPE, PMSA and

SIGY are strongly disturbed by ocean-generated noise. In contrast, excellent noise conditions were present at station BELO. During 1 yr of operation, 28 events with high-quality shear wave recordings could be used for the analysis. The reason for this is an almost optimal geographical location with respect to the main earthquake-generating regions and a low noise level due to a nearly entire year of sea ice cover of the southern Weddell Sea. At the temporary stations JUBY, ROTH and SIGY only one–three events could be used for the investigation due to short operation times and bad signal-to-noise ratios.

Fig. 5 shows splitting parameters of the stations where more than three data sets could be used. With the exception of HOPE, a sufficiently good azimuthal coverage for the stations is achieved. In the case of an idealized model of a single layer of seismic anisotropy with a horizontal symmetry axis, no variations of splitting parameters should occur for different azimuth and incident angles. Fig. 6 displays the single values for ϕ and δt and their dependence on initial polarization directions (backazimuth in the case of core phases). In most cases in which seismic anisotropy in the upper mantle was investigated, simplified station averages from many single measurements were determined (Vinnik *et al.* 1992; Wolfe & Silver 1998). These station averages may lead to misinterpretations in the case of strong azimuthal variations of the splitting parameters. Dependence on initial polarization direction may originate from more complex anisotropy systems such as layers with dipping symmetry axes, a pair of layers with different parameters of azimuthal anisotropy with horizontal symmetry axes, or more complex systems of intrinsic anisotropy such as orthorhombic systems (Plomerová *et al.* 1996).

For nearly all stations azimuthal variations of the splitting parameters do exist (Fig. 6). In the case of more complex anisotropy systems than those of a single-layer hexagonal anisotropy with horizontal symmetry axes, the parameters retrieved are apparent anisotropy parameters. From these apparent parameters more complex models may be constructed such as a two-layer model of azimuthal anisotropy. This model is described by Silver & Savage (1994). A linear polarized S wave is first split into two waves when it passes through the first layer and then further split into four waves when it passes through the second layer. Silver & Savage (1994) showed that the case of the inversion of splitting parameters under the assumption of a single layer is justified. The parameters retrieved from a one-layer assumption are apparent parameters, which may be fitted to a two-layer model with four independent parameters. From a geodynamic point of view such a model is reasonable, since both layers may correspond to anisotropy in the lithosphere and asthenosphere or distinct tectonic events that occurred at different depth levels. More complex anisotropy systems can only be developed from larger data sets from long observational times (Levin *et al.* 1999). Fig. 6 shows the azimuthal variations of the directly measured splitting parameters together with the fit of these apparent parameters to a two-layer model. The apparent splitting parameters are fitted by the four parameters $(\phi_1, \delta t_1, \phi_2, \delta t_2)$, with index 1 corresponding to the lower layer and index 2 to the upper layer. From appropriate selection of these parameters we attempted to fit the corresponding apparent parameters for each station. The fit was realized by essentially regarding the null directions and trends of variations of ϕ and δt values. In the case of two-layer anisotropy, apparent splitting parameters vary with a periodicity of 90° . For stations BELO, EFI, PMSA,

97/09/02 12:13:26.0 3.82N 75.74W 231 6.4 mb Colombia

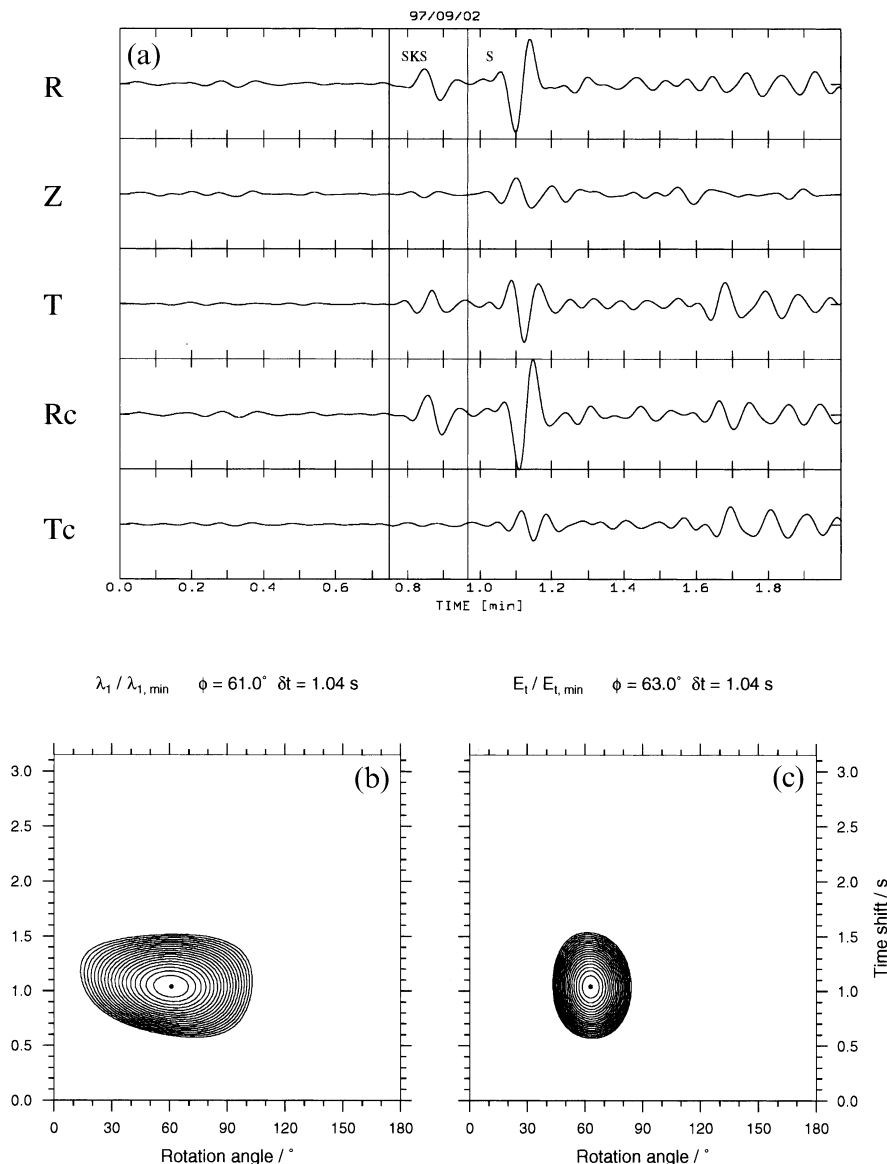
VNA3 (Neumayer/Soeraasen) Δ : 86.1 BAZ: 293.9

Figure 2. Example of *SKS* splitting analysis at station VNA3. (a) The top three seismograms show radial, vertical and transverse components, respectively. In the case of no anisotropy on the receiver path there should be no energy on the transverse component. The analysed time window is shown by vertical bars. The results of splitting analysis are shown underneath. From a net grid search analysis of the parameter space (ϕ , δt) the anisotropy parameters are determined by certain criteria [(b) minimizing the smaller of the eigenvalues of the horizontal covariance matrix; (c) minimizing the energy on the transverse component]. The contours show typical elliptical structures with well-constrained minima, typical of a high-quality splitting parameter estimation. Contour lines are normalized by the minimum values and displayed from 1 to 20. Since the dominant periods of teleseismic shear waves are around 8 s and typical delay times around $\delta t = 1$ s, no separated waves are observed but instead shear wave splitting is characterized by an elliptical particle motion. The lower two traces of the seismograms show the corrected radial and transverse components showing vanishing energy of the transverse *SKS* signal.

SNAA, VNA2 and VNA3, a sufficient number of measurements with good azimuthal coverage could be made for two-layer modelling. Taking into account these considerations, the two-layer fit to the data was performed manually and should serve as a first approximation to a model more complicated than just a single layer. The motivation for the choice of the individual parameters at each station will be discussed in the following section when discussing each station's anisotropic

properties. To avoid artefacts from non-receiver-side anisotropy, no *ScS* waves were used; only direct *S* waves, from earthquakes with hypocentres deeper than 200 km, were used. The large symbols in Fig. 6 show splitting parameters used primarily for two-layer estimations. Small symbols show splitting parameters of lower quality as well as *ScS* measurements.

A special case is the anisotropy investigations at the temporary station CAND (Candlemas, South Sandwich Islands,

98/06/07 13:01:16.2 15.959N 93.776W 87 6.3mb Near Coast of Chiapas, Mexico
 BELO (Belgrano II Station) Δ : 99.4 BAZ: 303.2

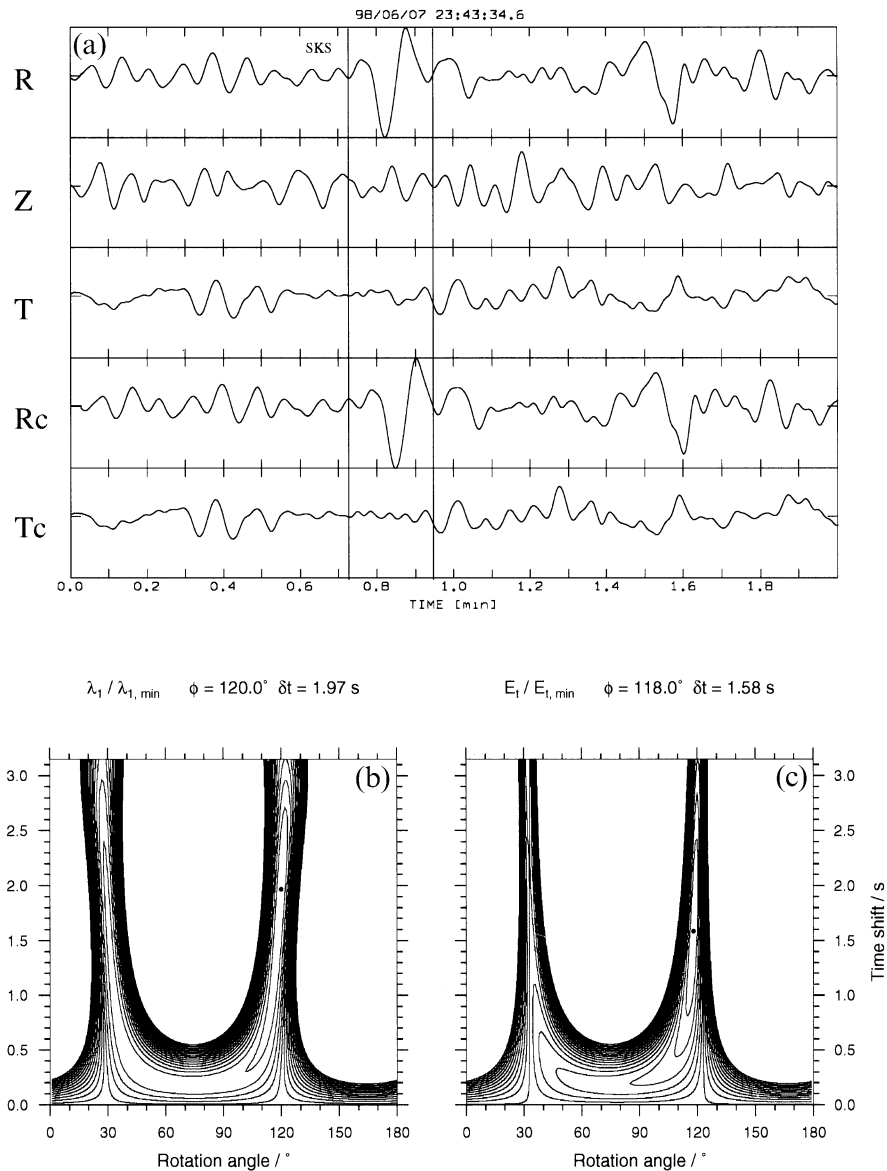


Figure 3. Same as Fig. 2 with an example for a null measurement at station BELO. The backazimuth (BAZ) and anisotropy symmetry axis coincide. The analysis is not stable and δt cannot be resolved. The delay time has no resolution and determination of the symmetry axis direction leads to two orthogonal minima. The seismogram shows that there is nearly no energy on the original transverse component. In this case the backazimuth (303°) and ϕ are separated by 83° , so are nearly orthogonal. The contour plot shows the typical U-shaped structure with minima separated by 90° .

Fig. 1). Here, no S waves from teleseismic events could be recorded with sufficient quality for estimating splitting parameters. A severe problem was the bad signal-to-noise ratio due to the close shoreline and bad weather conditions during the two months of operation. Nevertheless, six local earthquakes with hypocentres > 100 km were recorded, with direct S waves appropriate for splitting analysis. The retrieved splitting parameters (Fig. 7, shown at the corresponding epicentres) map the anisotropic structures of the lithospheric ray path between hypocentre and station. To obtain an estimate of the structure above the subducting South American Plate, where the anisotropy originates, the geometry of the plate was reconstructed from the distribution of relocated hypocentres according to

Engdahl *et al.* (1998). Fig. 7(b) shows the depth distribution of a 100-km-wide profile along the subduction direction. According to this simple local model, the largest part of the ray paths towards the station is situated in the lithosphere above the subducting plate. Fig. 8 shows the result of splitting measurements for event 980206b (Fig. 7).

Stations for which the receiver-side anisotropy structure is well known can be used for source-side studies of anisotropic structures. Records of S and S_cS waves may be corrected for the receiver anisotropy structures, and residual splitting parameters may be used for investigating source-side anisotropic structures (Barruol & Hoffmann 1999). Regarding the stations used in this contribution, VNA2 and VNA3 are candidates for

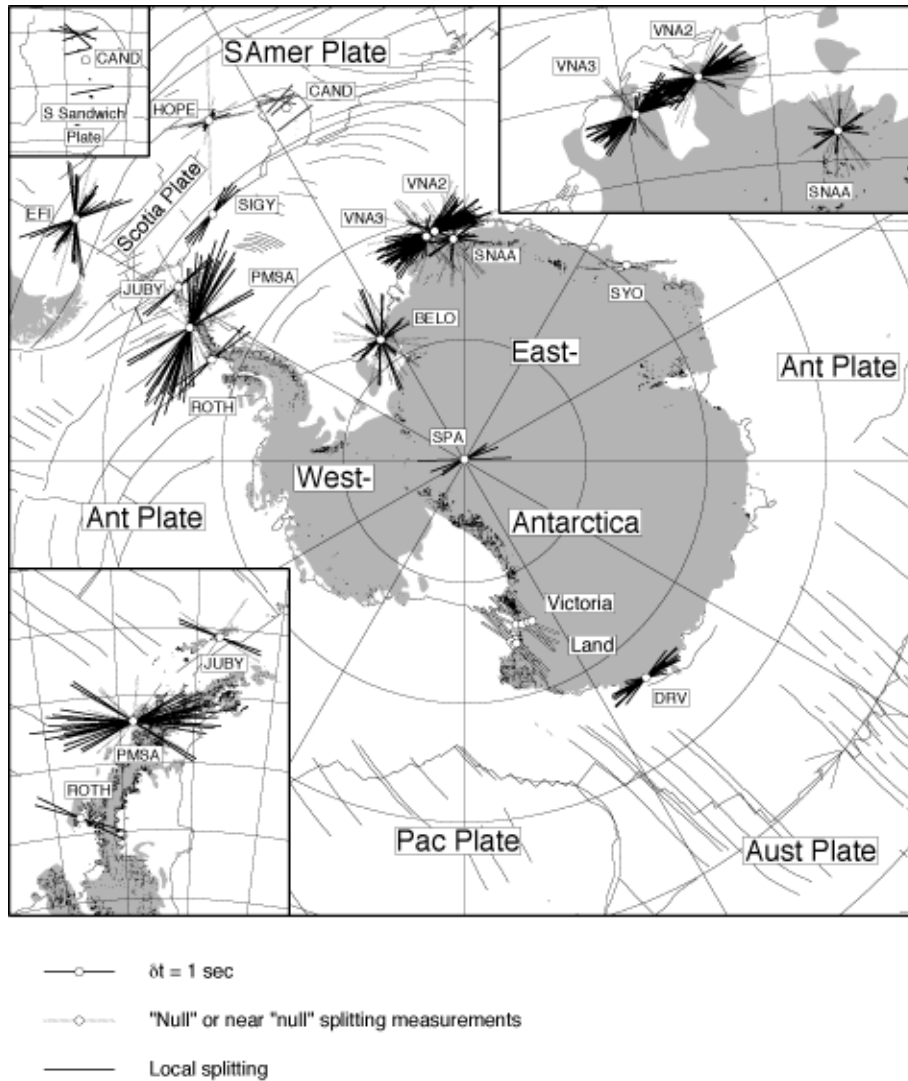


Figure 4. Splitting measurements carried out during this study. The bars show the directions of the fast polarization axis (ϕ) and their length is proportional to the delay times (δt). Polarization directions of null and near-null results are indicated by dashed lines in the fast and slow directions. The three insets show the splitting results of the South Sandwich Islands, Dronning Maud Land and Antarctic Peninsula regions enlarged. For local splitting observed at CAND, the fast polarization directions are shown at the corresponding epicentres. Additionally, the results of splitting analysis studies in Antarctica are shown for SYO (Syowa Station) from Kubo *et al.* (1995) and Victoria Land from Pondrelli & Azzara (1998).

source-side studies, since a large number of measurements exist and relatively weak azimuthal variations occur at these stations. In particular, the region beneath the slab of the South Sandwich subduction zone may be studied for the recent flow regime, since many *ScS* recordings of high quality exist that could be used for these studies. These investigations are of great interest, since the subduction is characterized by a strong slab roll-back (Barker 1995; Livermore *et al.* 1997), and horizontal mantle flows around the subducting plate may possibly be mapped.

3 SEISMIC ANISOTROPY AND REGIONAL TECTONICS

Investigations of seismic anisotropy in the Scotia Sea region are motivated by the assumption that the tectonic evolution of this region is influenced by mantle flows around South America from the Pacific into the Atlantic analogous to the Caribbean Plate tectonics in the north of the South American continent

(Alvarez 1982). The observation of such mantle flow sub-parallel to the subducting Nazca Plate, which is a barrier for the mantle flow regarding relative movement of the Nazca and South American plates, was proposed from splitting measurements (Russo & Silver 1994). In the Caribbean, this was also confirmed by anisotropy observations (Russo *et al.* 1996). The Scotia Sea region developed in the last 35 Myr after the opening of Drake Passage (Barker & Dalziel 1983) and is composed of fragments of continental and oceanic crust. The Antarctic Peninsula and South Shetland Islands are overprinted by eastward-directed subduction of the Pacific and proto-Pacific plates beneath the Antarctic plate, which came to rest from southwest to northeast by ridge-crest collision (Larter & Barker 1991). Today, subduction is believed to be still active only in the region between the Hero and Shackleton Fracture zones (Fig. 9a). The Antarctic Peninsula was formed by complex kinematic processes, by various shear, extensional and compressional events, often accompanied by magmatic extrusions (Storey *et al.* 1996).

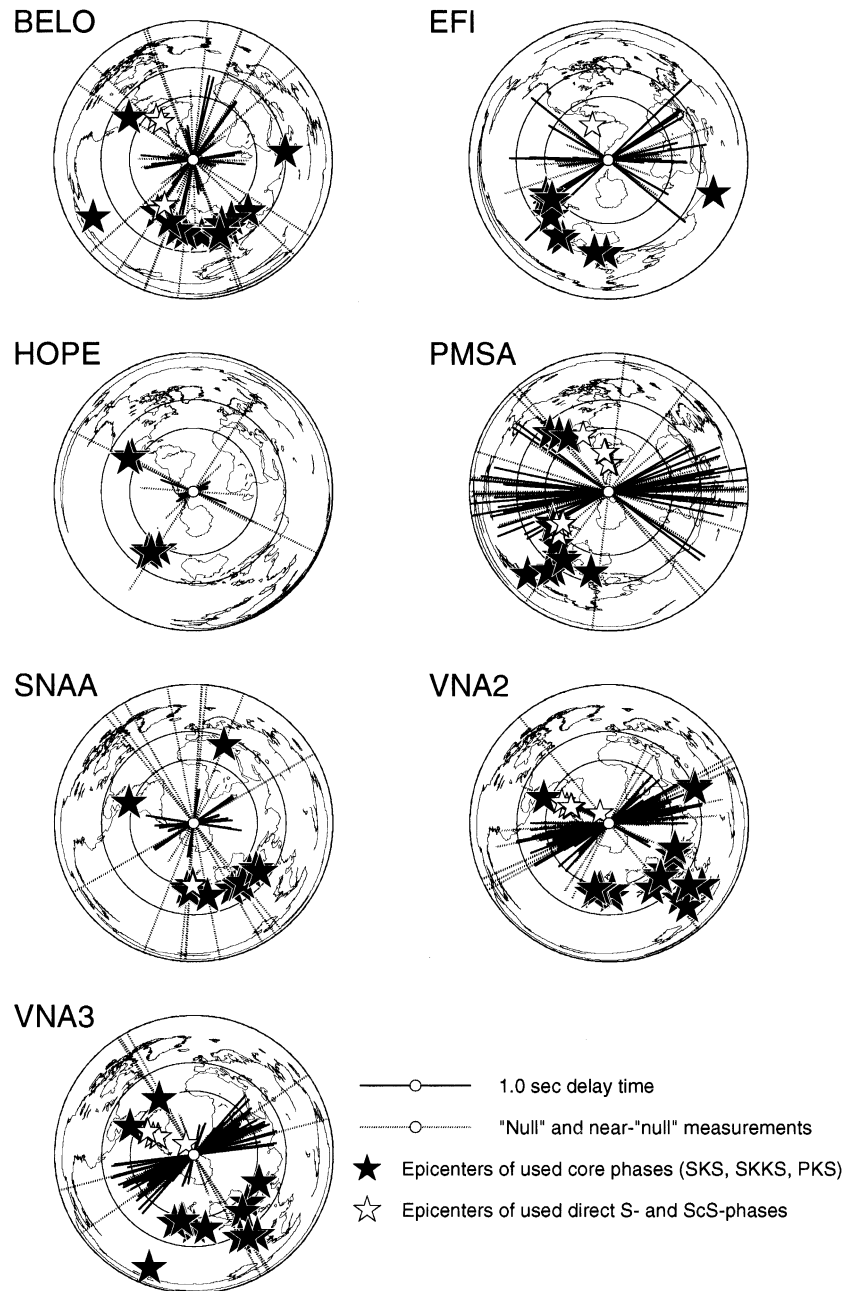


Figure 5. Measured fast polarization directions and delay times at stations with more than three observations. Additionally, the epicentres of the events used are shown in an azimuthal equidistant projection. The best distance range for recording *SKS* ($85^\circ < \Delta < 110^\circ$) is marked by circles.

With the exception of the northern Antarctic Peninsula, all Antarctic continental margins are passive margins. In the case of western Dronning Maud Land these are of volcanic type (White & McKenzie 1989). Western Dronning Maud Land and Coats Land (Fig. 10) were formed as part of the East Antarctic Craton by various tectonic events such as mountain building during the Grenvillian orogeny (1100 Ma), assembly of Gondwana by Panafrican overprinting (600 Ma) (Paech *et al.* 1991; Jacobs *et al.* 1998) and the disintegration of Gondwana (Martin & Hartnady 1986). For understanding the details of the break-up of Gondwana in particular, this region is of major interest. Break-up here started 170 Myr ago, possibly strongly influenced by the activity of the Bouvet mantle plume and effusion of the Karoo and Ferrar large igneous provinces

(Dalziel *et al.* 2000). These various geodynamic events are fairly well understood and investigations of seismic anisotropy in the underlying mantle will contribute to a better knowledge of these processes.

3.1 Antarctic Peninsula and Scotia Sea

Investigations of seismic anisotropy may contribute to ideas about the influence of recent mantle flows on the tectonic evolution of the Scotia Sea or how anisotropic structures in the lithosphere can be explained by such recent or fossil flow directions. In general, fast polarization axes in the Scotia Sea are E–W directed, with decreasing magnitudes of seismic

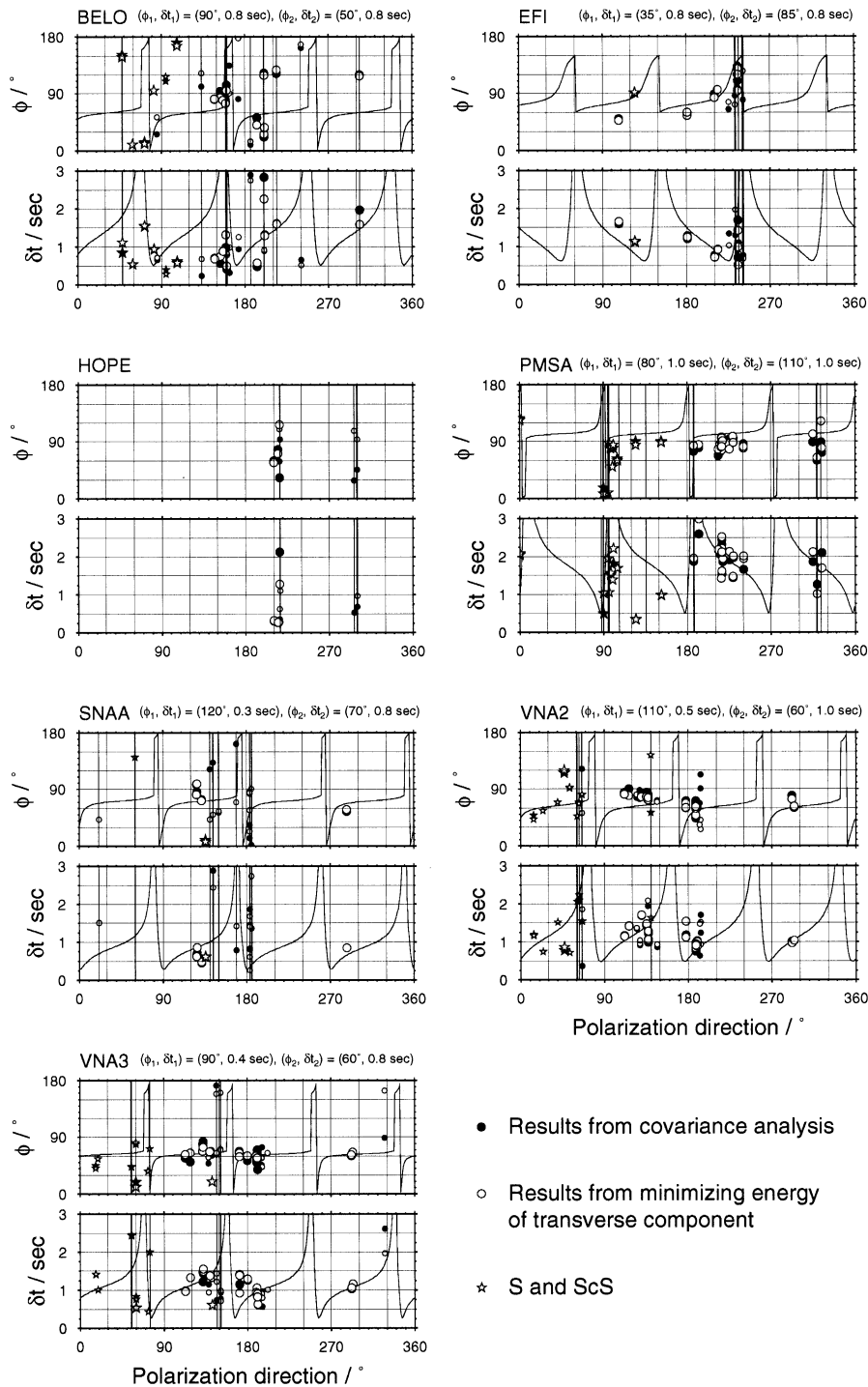


Figure 6. The anisotropy parameters ϕ and δt plotted against the initial polarization direction (backazimuth in the case of core phases). The directions of null measurements are indicated by vertical lines. At stations BELO, EFI, PMSA, SNAA, VNA2 and VNA3 the azimuthal variations of apparent splitting parameters are modelled by a two-layer case of anisotropy. The parameter pair $(\phi_1, \delta t_1)$ describes the lower and $(\phi_2, \delta t_2)$ the upper layer. Stars denote splitting measurements made from direct, deep-focus *S* and *ScS* waves. Small symbols are splitting parameters from poor-quality measurements as well as measurements from *ScS* waves.

anisotropy from west (PMSA: $\delta t = 1.8$ s) towards east (HOPE: $\delta t = 0.3$ s). Therefore, the direction ϕ corresponds to a postulated mantle flow from the Pacific (Alvarez 1982), but a lithospheric and therefore fossil part may not be excluded. In particular, the fact that nearly all stations, with the exception of CAND, are located on fragments of continental crust and exhibit delay times of $\delta t = 1.0$ s or less does not conclusively support an astheno-

spheric origin (Fig. 4). The only station where part of the anisotropy must be situated in the asthenosphere is station PMSA (Palmer Station), with a delay time of nearly 2 s. Here, for the understanding of azimuthal variations of the splitting parameters, two-layer model was applied. The azimuthal coverage is sufficient for two-layer modelling. Essentially, we tried to fit the null directions and variations of δt . For ϕ , the trend and the

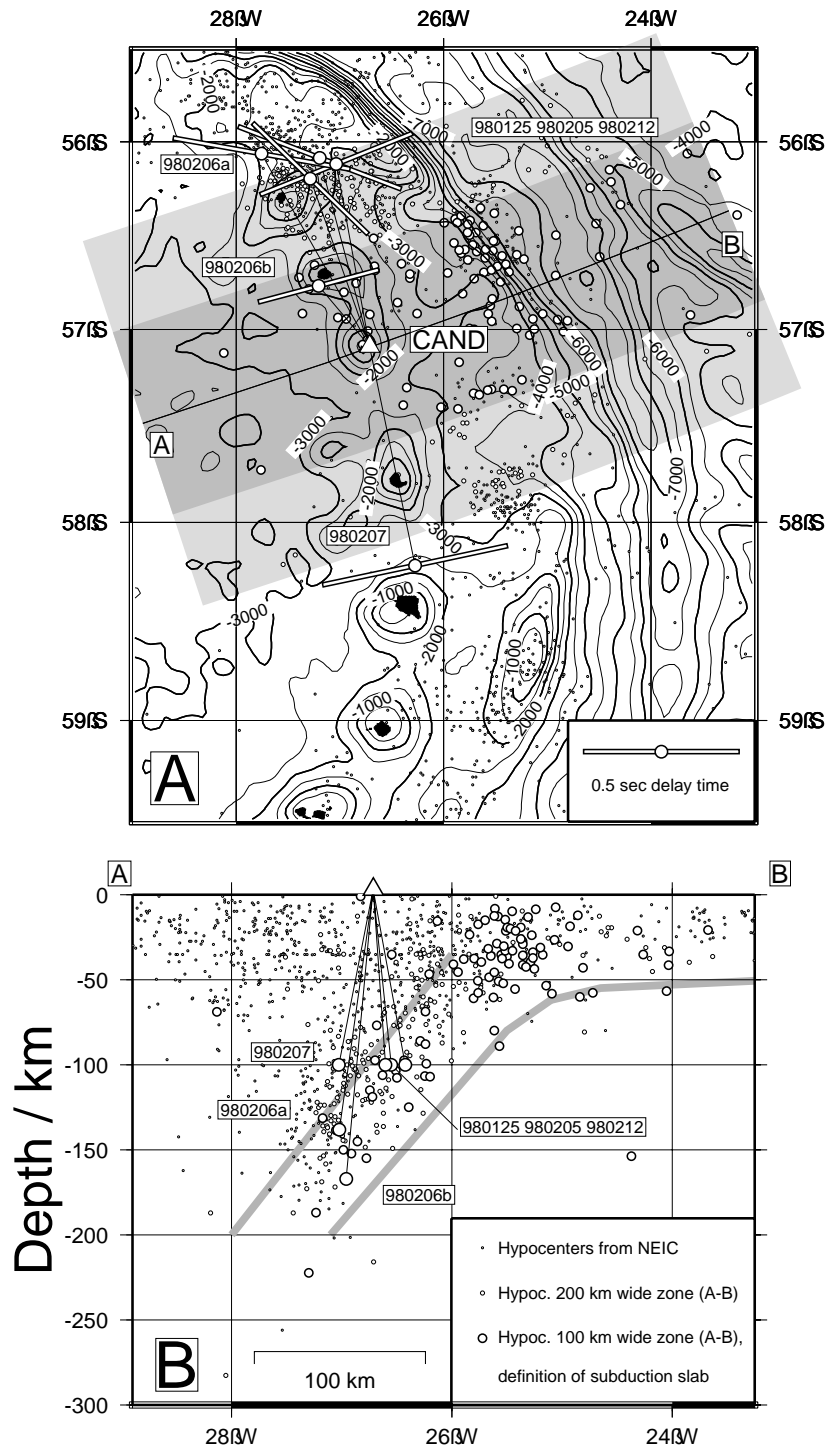


Figure 7. Seismic anisotropy in the lithosphere beneath station CAND, Candlemas Island, South Sandwich Islands. (a) Anisotropy parameters from direct, local *S* waves from deep hypocentres beneath the station. The anisotropy bars are plotted at the earthquake's epicentre, so they originate on the travel path between hypocentre and recording station. (b) For determination of the nature of the anisotropic source region, the geometry of the subducting plate was determined from the relocated hypocentres by Engdahl *et al.* (1998) along the profile A–B (see a).

90° jumps were fitted. Some results do not fit, indicating a more complex system (Fig. 6). The lithospheric part is, like the observations at JUBY and ROTH, ESE–WNW-directed. This direction is subparallel to the transform faults of the southeastern Pacific Plate, which continue into the Antarctic Peninsula (Hawkes 1981) and South Shetland Islands (Barker & Austin

1994). The direction of the lower, asthenospheric layer at PMSA has an ENE–WSW azimuth. This direction cannot be explained by a simple mantle flow pattern from the Pacific into the Scotia Sea. In fact, the subducted Phoenix Plate is also a barrier for asthenospheric mantle flows in this region. Simple calculations of the depth extent of the anisotropic layer are made from

98/02/06 13:01:16.2 56.059S 27.584W 128 5.5mb South Sandwich Islands Region
 CAND (Candlemas Island) Δ : 1.1 BAZ: 334.7

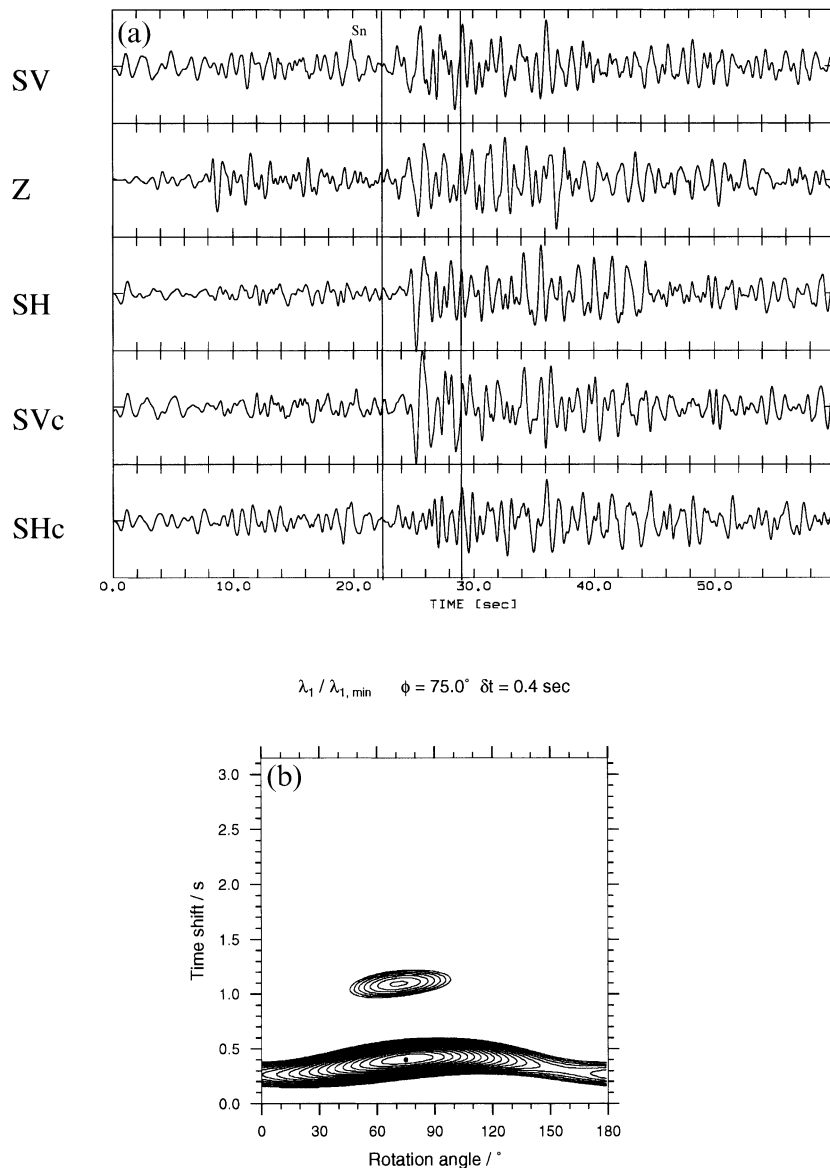


Figure 8. Same as Fig. 2 with an example of splitting analysis of a local S wave from a deep-focus event beneath the station CAND. Traces are filtered between 0.5 and 1.0 Hz. Nevertheless, some aliasing occurs as can be seen in the contour plot. The original and corrected horizontal components are rotated to the SV and SH components according to the initial polarization direction.

the relationship $L = \delta t \beta_0 / \delta \beta$, where L is the thickness of the anisotropic layer, $\beta_0 = 4.4 \text{ km s}^{-1}$ is the average shear wave velocity of the upper mantle, and $\delta \beta$ is the dimensionless S -wave anisotropy coefficient in per cent. Given a conservative estimate of the anisotropic layer thickness by assuming a high anisotropy coefficient of $\delta \beta = 5$ per cent, the depth extent is calculated for $\delta t = 1.8 \text{ s}$ (PMSA) to be $L = 160 \text{ km}$. According to Šroda *et al.* (1997), crustal thickness beneath PMSA is 40 km and lithospheric thickness should not greatly exceed 100 km. In fact, the Antarctic Peninsula stations (JUBY, PMSA, ROTH) are continental margin stations rather than purely continental, and therefore no extraordinary lithospheric thickness should be expected. Thus, due to the magnitude of seismic anisotropy, parts

of the source region are likely to be produced in the asthenosphere by recent mantle flow. This assumption supports the theory of Barker & Austin (1998), who proposed mantle flow in a northeasterly direction through a slab window of the subducted Phoenix Plate into the Weddell Sea (Fig. 9b). In addition, these findings are also supported by the Pacific-like origin of magmas at the northeastern Antarctic Peninsula and South Shetland Islands (Veit & Miller 1999).

At SIGY (Signy Island) the fast polarization direction corresponds to the strike of the South Scotia Transform Fault and has been produced by shear deformations. Averaged splitting parameters at EFI (East Falkland Island) are E–W directed and with $\delta t = 1.10 \text{ s}$ correspond to the global mean.

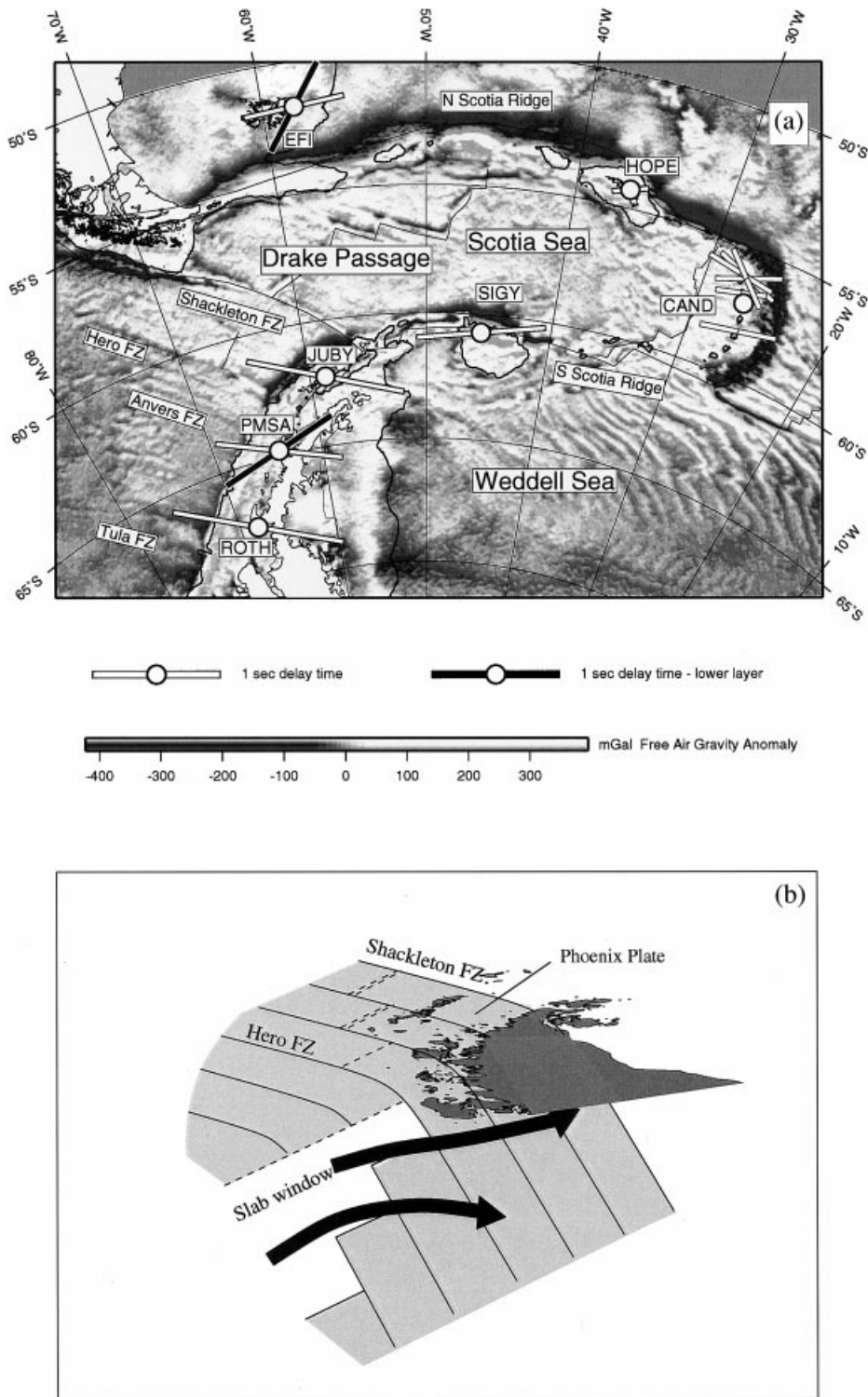


Figure 9. (a) Anisotropy parameters in the Scotia Sea and Antarctic Peninsula regions superimposed on free-air gravity anomalies from McAdoo & Laxon (1997). The splitting parameters are averaged and in the cases of EFI and PMSA those of the upper and lower layers are shown. In general, fast anisotropy directions are E–W directed and the magnitude of anisotropy decreases from W towards E. (b) A proposed model for the exceptionally high δt values observed at PMSA following Barker & Austin (1998). High δt values and directions are explained by an actual asthenospheric flow through a slab window above the subduction slab of the former Phoenix Plate.

This direction corresponds to an asthenospheric flux as proposed by Alvarez (1982). Nevertheless, a strong azimuthal variation of measurements exists. Modelling of two anisotropic layers is possible from a fairly good azimuthal coverage

(Fig. 6). This leads to fast polarization directions of the upper layer of $\phi_2=85^\circ$ and a lower layer fast direction of $\phi_1=35^\circ$, which is not compatible with the proposed asthenospheric flow direction. This result agrees with splitting parameters derived

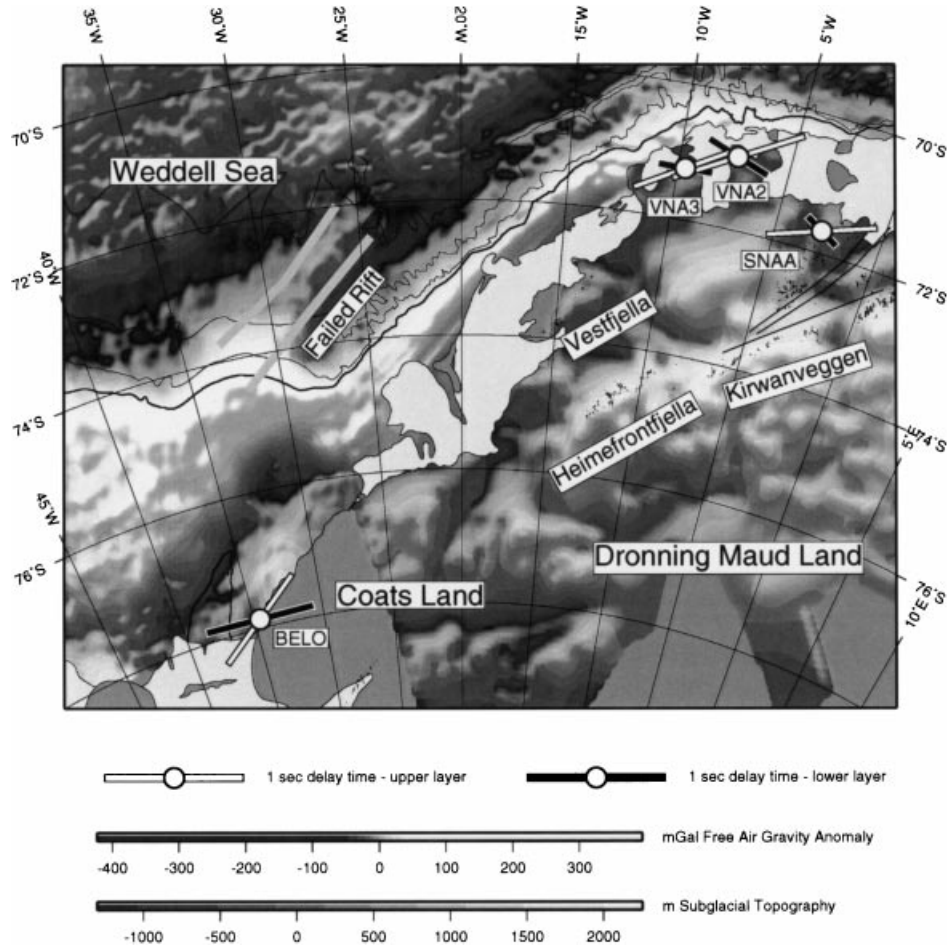


Figure 10. Two-layer anisotropy in Dronning Maud and Coats Land. At all stations (BELO, SNAA, VNA2 and VNA3) the upper layer is parallel to the passive continental margin and was formed by early mountain building episodes (Grenvillian, Panafrican) or even earlier as part of the Kaapvaal Craton. The lower layer may have been created during early rifting events of the Gondwana disintegration. The directions are subparallel to large-scale features [free-air gravity anomaly from Schöne & Schenke (1997); subglacial topography from Steinhage *et al.* (1999)].

from a temporary experiment in Patagonia (Helffrich *et al.* 1997). In particular, these directions contradict the hypothesis of mantle flow into the Scotia Sea, and the source of anisotropy likely in the lithosphere. The lower layer direction corresponds to the strike of the Falkland Sound Fault (Marshall 1994), separating the two main islands, while the upper layer direction corresponds to structural trends of northern East Falkland (Greenway 1972). This upper layer direction corresponds to the Jurassic extension of the Falkland Platform and Maurice Ewing Bank east of the Falkland Platform (Marshall 1994). HOPE (South Georgia) shows anomalous small delay times (stable measurements averaged $\delta t = 0.3$ s) and is not stable from single measurements. An azimuthal variation could not be resolved, since only events from two narrow azimuthal sectors could be used (Fig. 6). These azimuths are near the symmetry directions and perpendicular. The ϕ and null directions are consistent. Since South Georgia is a fragment of an old island arc, the fast direction corresponds to the former subduction direction. Subduction processes probably stopped here 7–10 Myr ago (Barker 1995). A complex tectonic history with a variety of structures may decrease the delay times.

At CAND (Candlemas Island), the retrieved splitting parameters deduced from direct *S* splitting are in the range $0.4 < \delta t < 0.6$ s and the fast polarization axes are E–W directed.

The smallest delay time ($\delta t = 0.4$ s) was estimated for an event with the largest hypocentral depth and occurred nearly below the recording station (Fig. 8). Because of the large depth it should have the largest delay time. A large part of the ray path of this event traverses the subducting plate and may be influenced by possible anisotropy of different structures, which may decrease the total delay time. Another explanation for the larger δt of the other investigated events may be the station–epicentre geometry, since the rays are no longer vertical in these cases. The ϕ directions of the northern events show more NW–SE-directed parts. This might be an effect of deformation of the lithosphere in the transition regime between subduction and transform faults. Previously investigated anisotropy in subduction zones led to a variety of different fast polarization directions with respect to the subduction geometry. These different results are attributed to distinct regions traversed by the *S* waves, above, below and inside the subduction slab, or to specific features of the subduction regime. In strained back-arc regions, as in this case, ϕ directions were found subparallel to the extension direction of the back-arc spreading centres [Kurile Islands—Fischer & Yang (1994); Fiji Islands—Fischer & Wiens (1996) and Bowman & Ando (1987); Marianas—Fouch & Fischer (1998) and Xie (1992); Tonga and Izu-Bonin—Bowman & Ando (1987), Fischer & Wiens (1996) and Fouch &

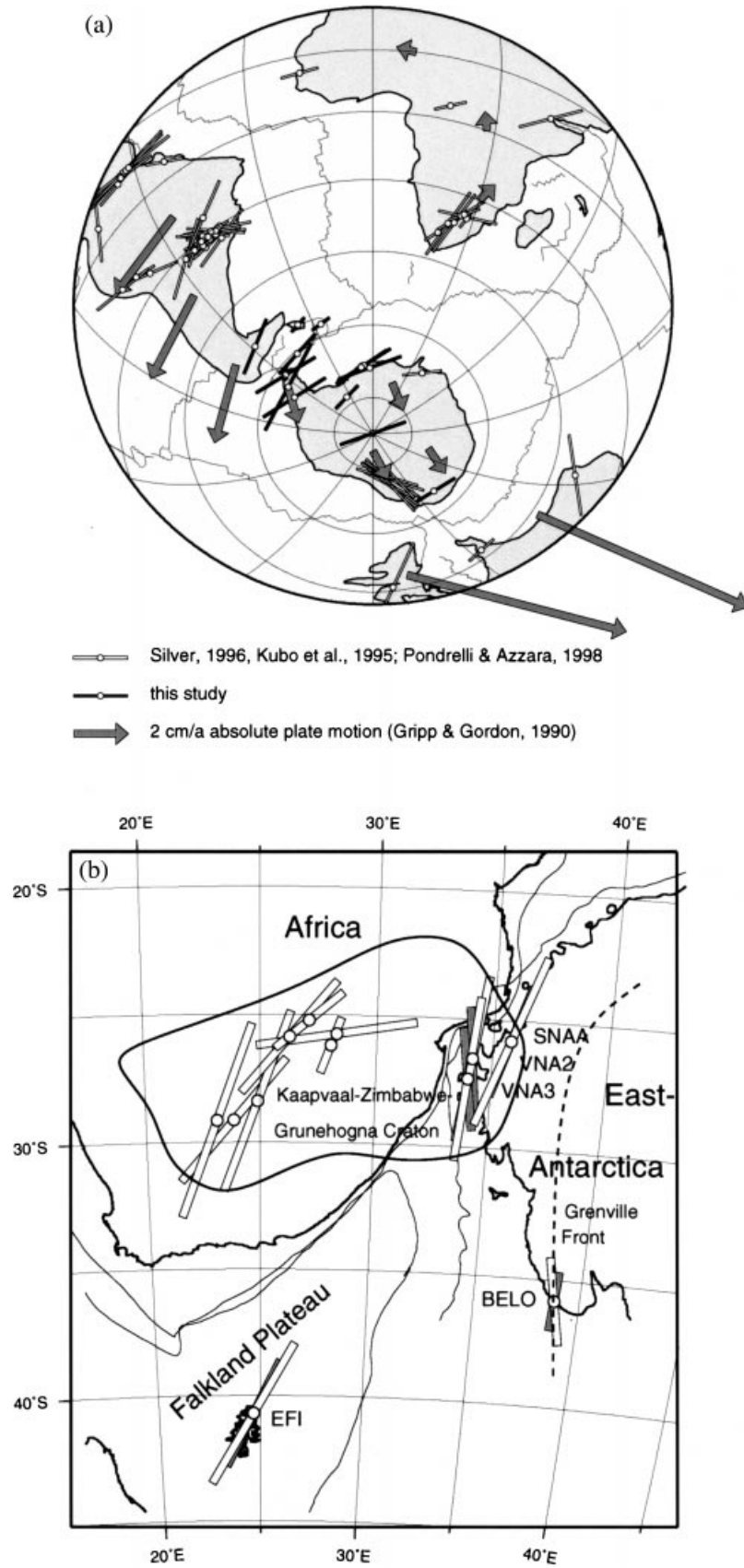


Figure 11. Comparison of seismic anisotropies (fast directions) in Antarctica with those of Africa and South America in present-day configuration together with absolute plate motions (a) and in a simple Gondwana reconstruction (b) following Martin & Hartnady (1986) in an African reference frame. Schematically, the boundary of the Kaapvaal–Zimbabwe–Grunehogna Craton and the East Antarctic Grenville Front are included. Here, for BELO, EFI, SNAA, VNA2, and VNA3, averaged splitting parameters (white bars) and upper layer (grey bars) parameters are shown.

Fischer (1996)]. Due to the known lithospheric travel path of the wave an estimation of anisotropy strength is possible. The strength of seismic anisotropy in these observations is 0.9–1.5 per cent, corresponding to the globally observed values. These results compare very well with other investigations in back-arc spreading zones such as the Northwest Pacific (0.5–1.1 per cent; Fouch & Fischer 1996) and the Aleutian Islands (1.0 per cent; Yang *et al.* 1995). The fast direction corresponds to the back-arc rifting direction of the East Scotia Ridge with a current opening rate of 65–70 km Myr⁻¹ (Livermore *et al.* 1997). The South Sandwich microplate is characterized by a rapid eastward movement and a corresponding roll-back of the subducting slab (Barker 1995; Barker *et al.* 1991).

Another possible explanation for the origin of seismic anisotropy is absolute plate motion (APM) with respect to a hotspot-fixed reference system. Differential movements between asthenosphere and the overlying lithosphere probably generate anisotropic structures in the direction of movement (Vinnik *et al.* 1992). Fig. 11(a) shows the APM directions according to the model of Gripp & Gordon (1990). Only at EFI are polarization directions close to the APM directions; in general, delay times and plate velocities are poorly correlated.

3.2 Western Dronning Maud and Coats Land

At station BELO, in general small delay times ($\delta t < 0.5$ s) were measured. In the case of weak anisotropy the methods used tend to be less stable. Therefore, the results of the single measurements are strongly variable, although the recordings at this station are of high quality (Fig. 6). However, a systematic azimuthal variation of apparent parameters could be observed and as a first approximation a two-layer model is constructed (Fig. 6) with an upper layer parallel to the continental margin and the lower layer oriented in an E–W direction (Fig. 10). Nevertheless, it is likely that a more complex anisotropy system exists. The eastern continental margin of the Weddell Sea in this region was influenced by volcanic extrusions during Gondwana break-up processes and was strongly extensional at that time, resulting in a ‘failed rift’ structure parallel to the continental margin (Kristoffersen & Hinz 1991), possibly continuing in a SSW direction into the Filchner Shelf. In addition, Precambrian structures, evident from the Bertrab–Littlewood–Moltke Nunataks (Marsh & Thomson 1984) volcanic outcrops where BELO is situated, suggest complex anisotropic structures formed by these various dynamic processes. In particular, the Grenville Front, a suture separating the East Antarctic Craton in the south from the deformational provinces in the north (Storey *et al.* 1994) is situated in this region. According to Jacobs (1998), the Grenville Front is located just north of the Bertrab–Littlewood–Moltke Nunataks, which are therefore underlain by cratonic crust. The fast anisotropy directions (averaged and upper layer) follow the strike of the proposed Grenville Front (Fig. 11b). As described above, the measurements at BELO are generally of good quality, and future measurements will help in the construction of a refined model of anisotropy. Since this station fills a large gap in Antarctic station distribution, it was decided to convert BELO from a temporary to a permanent site within the framework of an Argentine–German co-operation.

At stations VNA2 and VNA3, two-layer models could be derived that fit the apparent parameters sufficiently well (Fig. 6).

The structures at both stations are quite similar. Splitting parameters for both stations show few differences. Also, for these stations, the main emphasis while fitting the data to a two-layer model was the best approximation of the position of null directions and the trends of the data. The splitting parameters at SNAA are not as clear as those of VNA2 and VNA3. A similar model was chosen as for VNA2 and VNA3. The fit is not as good as for the other two stations. In particular, the fit of null directions shows no 90° periodicity. A more complex anisotropy structure at SNAA seems likely. All stations in this region show evidence for more complex anisotropic structures. Two-layer models could be constructed for stations BELO, SNAA, VNA2 and VNA3 (Fig. 10). In general, the upper layers are parallel to the continental margins and large-scale geological features such as gravity anomalies (Jokat *et al.* 1996) or the strike of the mountain ranges of Vestfjella, Heimefrontfjella and Kirvanveggen. Within the context of mountain building episodes, fast polarization directions align with transpressional mechanisms parallel to the strike of mountain chains as a consequence of vertical coherent deformation of the underlying mantle (Barruol *et al.* 1998; Nicolas 1993; Silver 1996). A schematic reconstruction of Gondwana (Fig. 11b) shows the strike of anisotropy directions aligned with the continental margin of the eastern Weddell Sea, the Kaapvaal Craton in South Africa and the Falkland Plateau (EFI). This observation supports the idea that part of Dronning Maud Land, named the Grunehogna Craton, was part of the Kaapvaal–Zimbabwe–Grunehogna Craton (Fig. 11b), which was separated from Africa during Gondwana break-up (Moyes *et al.* 1993). These findings are supported by geological and magnetic observations in both South Africa and Dronning Maud Land (Corner & Groenewald 1981). In that case, anisotropic structures in this depth range are of Precambrian origin. A similar observation was made by Barruol *et al.* (1997), who investigated anisotropic structures on both margins of the northern Atlantic and explained with the Archaean roots of Pangea. The upper layer fast direction of EFI also fits this reconstruction, but it must be considered a rotation about 180° from its pre-drift position near the South African Cape Fold Belt (Marshall 1994).

Fast polarization directions of the lower layers show consistent results at all four stations. These are rotated about 30° relative to the strike of the continental margin (Fig. 10). These structures might have been produced from a younger tectonic event, presumably being connected to rifting episodes during the initial break-up of Gondwana (Fig. 11b). Rift-related anisotropy is mainly subparallel to the strike of the rift system and may originate from the freezing of upwelling mantle material along the rift walls during rifting episodes (Nicolas 1993; Gao *et al.* 1997; Vauchez *et al.* 1997; Vauchez *et al.* 2000), but it could also result from a variety of other processes. Continental rifts often develop from pre-rift-generated deformation such as that associated with a former orogenesis (Vauchez *et al.* 1997) and modify pre-existing lithospheric fabrics by transcurrent, rift-parallel lithospheric deformation during the rifting process, associated asthenospheric flow—mainly observed as being parallel to the strike of the rift—and development of melt-filled pockets in the asthenospheric wedge of the rift (Vauchez *et al.* 2000). These processes, when compared with anisotropy structures at Dronning Maud and Coats Land, favour the origin of the anisotropy as ancient lithospheric structure modified by rifting processes during Gondwana break-up.

3.3 East Antarctica

At SPA only two events were found that were appropriate and of sufficient quality for splitting analysis. This seems to be unusual for this station since it has the longest operation time of all the stations used. A possible explanation for the insufficient quality of the *S* waveforms is the influence of the 3 km thick ice sheet underlying the station. Seismic anisotropy at SPA ($\delta t = 1.28$ s) cannot be explained by APM, nor by mountain building of the Transantarctic Mountains. In the latter case, the fast polarization directions should align with the strike of the mountain range. In comparison, the lithospheric roots beneath the North American shield show relatively strong anisotropy effects, which originated in Precambrian times (Silver & Chan 1991).

In general, the fast polarization directions follow the strike of the continental margins of East Antarctica (Fig. 11a). The fast directions do not agree with recent APM directions according to the model of Gripp & Gordon (1990). The delay times at DRV (0.9 s) and SYO (0.7 s) are slightly below the global average of 1.0 s (Silver 1996). Kubo *et al.* (1995) discuss anisotropy at SYO as originating from palaeomantle flows. Splitting parameters retrieved at DRV agree with those of Barruol & Hoffmann (1999). The authors discuss a two-layer structure from a slight azimuthal variation but do not discuss a geodynamic interpretation. Anisotropy in Victoria Land is explained by structures that originated from processes connected with the opening of the Ross Sea, a still active rift system (Pondrelli & Azzara 1998). In general, fast polarization directions around the passive margins of Antarctica discussed here follow the strike of the coastlines. This might be explained by recent mantle flow around the continental keel of the East Antarctic Craton. Similar flows were recently modelled for eastern North America by Fouch *et al.* (2000). Nevertheless, since only very slow APM velocities occur for East Antarctica this model seems to be unlikely for this continent. A better explanation of this obvious parallelism of anisotropy and coastlines in East Antarctica is the coherence of rifted margins and anisotropy (Vauchez *et al.* 1997; Vauchez *et al.* 2000) discussed above.

4 CONCLUSIONS

Investigations of seismic anisotropy in the Scotia Sea region and along the Antarctic Peninsula, the passive continental margin of the eastern Weddell Sea and stations on the East Antarctic Craton give new insights into the structure of the upper mantle and indications of the historical and recent tectonic evolution.

In the Antarctic Peninsula and Scotia Sea, anisotropy models support the hypothesis of asthenospheric flow from the Pacific into the Atlantic according to Alvarez (1982). The interpretations still remain partly speculative, but in the Scotia Sea and Antarctic Peninsula fast polarization directions (in general E–W) do not contradict this hypothesis. Since the methods used do not resolve the depth at which the seismic anisotropy occurs, a lithospheric part may also be responsible for the splitting parameters derived. However, recent flow around the southwestern edge of the subducting Phoenix Plate explains the strong anisotropy and its directions at PMSA, which influences the tectonics in the region of the Bransfield Strait.

The mapping of anisotropic structures allows the continuation of geological structures into the Earth's upper mantle. In particular, in parts of Antarctica where a direct mapping of geological structures is not possible due to the ice cover, investigations of seismic anisotropy give indications of the tectonic evolution of these regions. In western Dronning Maud and Coats Land, the anisotropy is explained as originating from the influence of tectonic events in Precambrian times, overprinted by initial rifting during the break-up of Gondwana.

ACKNOWLEDGMENTS

The ideas for this research were developed together with Alfons Eckstaller and Wilfried Jokat. I gratefully acknowledge their support concerning logistical assistance and scientific discussions. Instituto Antártico Argentino and the British Antarctic Survey provided support and maintenance for using their sites. I wish to thank two anonymous reviewers for their helpful reviews of the manuscript and Peter F. Barker for giving valuable suggestions on interpretation of anisotropy regarding Scotia Sea evolution. I thank Gabi Uenzelmann-Neben for improving the style of this manuscript. Figures were created using the GMT graphics package (Wessel & Smith 1998). This research was partly funded by the German Bundesministerium für Bildung, Forschung und Technologie under grant No 03PL022G. This is Alfred Wegener Institute contribution No. AWI-N10128.

REFERENCES

- Alvarez, W., 1982. Geological evidence for the geographical pattern of mantle return flow and the driving mechanism of plate tectonics, *J. geophys. Res.*, **87**(B8), 6697–6710.
- Barker, D.H.N. & Austin, J.A., 1994. Crustal diapirism in Bransfield Strait, West Antarctica: evidence for distributed extension in marginal-basin formation, *Geology*, **22**, 657–660.
- Barker, D.H.N. & Austin, J.A., 1998. Rift propagation, detachment faulting, and associated magmatism in Bransfield Strait, Antarctic Peninsula, *J. geophys. Res.*, **103**(B10), 24 017–24 043.
- Barker, P.F., 1995. Tectonic framework of the east Scotia Sea, in *Back-arc Basins: Tectonics and Magmatism*, pp. 281–248, ed. Taylor, B.J., Plenum Press, New York.
- Barker, P.F. & Dalziel, I.W.D., 1983. Progress in the dynamics of the Scotia Sea Region, in *Geodynamics of the Eastern Pacific Region, Caribbean and Scotia Arcs*, *AGU Geodyn. Ser.*, **9**, 137–170.
- Barker, P.F., Dalziel, I.W.D. & Storey, B.C., 1991. Tectonic evolution of the Scotia Sea region, in *Antarctic Geology*, pp. 215–248, ed. Tingey, J.R., Oxford University Press, Oxford.
- Barruol, G. & Hoffmann, R., 1999. Upper mantle anisotropy beneath the GEOSCOPE stations, *J. geophys. Res.*, **104**(B5), 10 757–10 773.
- Barruol, G., Helffrich, G. & Vauchez, A., 1997. Shear wave splitting around the Northern Atlantic: frozen Pangaeian anisotropy?, *Tectonophysics*, **279**, 135–148.
- Barruol, G., Souriau, A., Vauchez, A., Diaz, J., Gallart, J., Tubia, J. & Cuevas, J., 1998. Lithospheric anisotropy beneath the Pyrenees from shear wave splitting, *J. geophys. Res.*, **103**(B12), 30 039–30 053.
- Ben Ismail, W. & Mainprice, D., 1998. An olivine fabric database: an overview of upper mantle fabrics and seismic anisotropy, *Tectonophysics*, **296**, 145–157.
- Bowman, J.R. & Ando, M., 1987. Shear-wave splitting in the upper-mantle wedge above the Tonga subduction zone, *Geophys. J. R. astr. Soc.*, **88**, 25–41.
- Corner, B. & Groenewold, P.B., 1991. Gondwana reunited, *S. African J. Antarctic Res.*, **21**, 172.

- Dalziel, I.W.D., Lawver, L.A. & Murphy, J.B., 2000. Plumes, orogenesis, and supercontinental fragmentation, *Earth planet. Sci. Lett.*, **178**, 1–11.
- Dietrich, R., 2000. Deutsche Beiträge zu GPS-Kampagnen des Scientific Committee on Antarctic Research (SCAR) 1995–1998, *Deutsche Geodätische Kommission bei der Bayerischen Akademie der Wissenschaften*, Reihe B, **310**, München.
- Engdahl, E.R., van der Hilst, R.D. & Buland, R.P., 1998. Global teleseismic earthquake relocation with improved travel times and procedures for depth determination, *Bull. seism. Soc. Am.*, **88**, 722–753.
- Fischer, K.M. & Wiens, D.A., 1996. The depth distribution of mantle anisotropy beneath the Tonga subduction zone, *Earth planet. Sci. Lett.*, **142**, 253–260.
- Fischer, K.M. & Yang, X., 1994. Anisotropy in Kuril-Kamchatka subduction zone structure, *Geophys. Res. Lett.*, **21**, 5–8.
- Fouch, M.J. & Fischer, K.M., 1996. Mantle anisotropy beneath north-west Pacific subduction zones, *J. geophys. Res.*, **101**, 15 987–16 002.
- Fouch, M.J. & Fischer, K.M., 1998. Shear wave anisotropy in the Mariana subduction zone, *Geophys. Res. Lett.*, **25**, 1221–1224.
- Fouch, M.J., Fischer, K.M., Parmentier, E.M., Wyssession, M.E. & Clark, T.J., 2000. Shear wave splitting, continental keels, and patterns of mantle flow, *J. geophys. Res.*, **105**(B3), 6255–6275.
- Gao, S., *et al.*, 1997. SKS splitting beneath continental rift zones, *J. geophys. Res.*, **102**(B10), 22 781–22 797.
- Greenway, M.E., 1972. The geology of the Falkland Islands, *Br. Antarct. Surv. Sci. Rept.*, **76**.
- Gripp, A.E. & Gordon, R.G., 1990. Current plate velocities relative to the hotspots incorporating the NUVEL-1 global plate motion model, *Geophys. Res. Lett.*, **17**, 1109–1112.
- Hawkes, D.D., 1981. Tectonic segmentation of the northern Antarctic Peninsula, *Geology*, **9**, 220–224.
- Helfrich, G., Wiens, D.A., Barrientos, S. & Vera, E., 1997. Mantle flow through the Drake Passage: teleseismic shear wave splitting results from the SEPA experiment, *EOS, Trans. Am. Geophys. Un.*, **78**, 708.
- Jacobs, J., 1998. Tectono-thermal correlation of Grenville-age crust in SE-Africa, the Falkland microplate and East Antarctica and their contrasting Pan-African overprint, *habilit thesis*, Bremen University.
- Jacobs, J., Fanning, C., Henjes-Kunst, F., Olesch, M. & Paech, H.-J., 1998. Continuation of the Mozambique Belt into East Antarctica: Grenville-age metamorphism and polyphase Pan-African high-grade events in Central Dronning Maud Land, *J. Geol.*, **106**, 385–406.
- Jokat, W., Hübscher, C., Meyer, U., Oszko, L., Schöne, T., Versteeg, W. & Miller, H., 1996. The continental margin off East Antarctica between 10°W and 30°W, in *Weddell Sea Tectonics and Gondwana Break-up*, eds Storey, B.C., King, E.C. & Livermore, R.A., *Geol. Soc. Lond. Spec. Publ.*, **108**, 129–141.
- Kennett, B.L.N., 1995. Seismic traveltimes tables, in *Global Earth Physics. A Handbook of Physical Constants*, AGU Ref. Shelf., Vol. 1, pp. 126–143, ed. Ahrens, T.J., AGU, Washington, DC.
- Kristoffersen, Y. & Hinz, K., 1991. Evolution of the Gondwana plate boundary in the Weddell Sea area, in *Geological Evolution of Antarctica*, pp. 225–230, eds Thomson, M.R.A., Crame, J.A. & Thomson, J.W., Cambridge University Press, Cambridge.
- Kubo, A., Hiramatsu, Y., Kanao, M., Ando, M. & Terashima, T., 1995. An analysis of the SKS splitting at Syowa Station in Antarctica, *Proc. NIPR Symposium on Antarctic Earth Sciences*, **8**, 25–34, National Institute of Polar Research, Tokyo.
- Larter, R.D. & Barker, P.F., 1991. Effects of ridge-crest trench interaction on Antarctic-Phoenix spreading: forces on a young subducting plate, *J. geophys. Res.*, **96**, 19 583–19 607.
- Levin, V., Menke, W. & Park, J., 1999. Shear wave splitting in the Appalachians and the Urals: a case for multilayered anisotropy, *J. geophys. Res.*, **104**(B8), 17 975–17 993.
- Livermore, R., Cunningham, A., Vanneste, L. & Larter, R., 1997. Subduction influence on magma supply at the East Scotia Ridge, *Earth planet. Sci. Lett.*, **150**, 261–275.
- Mainprice, D. & Silver, P.G., 1993. Interpretation of SKS-waves using samples from the subcontinental lithosphere, *Phys. Earth planet. Inter.*, **78**, 257–280.
- Mainprice, D., Barruol, G. & Ben Ismail, W., 2000. The seismic anisotropy of the earth's mantle: from single crystal to polycrystal, in *Earth's Deep Interior: Mineral Physics and Tomography from the Atomic to Global Scale*, ed. Karato, S.I., *AGU Geophys. Monogr.*, **117**, 237–263.
- Marsh, P.D. & Thomson, J.W., 1984. Location and geology of nunataks in north-western Coats Land, *Br. Antarct. Surv. Bull.*, **65**, 33–39.
- Marshall, J.E.A., 1994. The Falkland Islands: a key element in Gondwana paleogeography, *Tectonics*, **13**, 499–514.
- Martin, A.K. & Hartnady, C.J.H., 1986. Plate tectonic development of the southwest Indian Ocean: a revised reconstruction of East Antarctica and Africa, *J. geophys. Res.*, **91**, 79–96.
- McAdoo, D.C. & Laxon, S.W., 1997. Antarctic tectonics: constraints from an ERS-1 satellite marine gravity field, *Science*, **276**, 556–561.
- Moyes, A.B., Barton, J.M. & Groenewald, P.B., 1993. Late Proterozoic to Early Paleozoic tectonism in Dronning Maud Land, Antarctica, *J. geol. Soc. Lond.*, **150**, 833–842.
- Nicolas, A., 1993. Why fast polarization directions of SKS seismic waves are parallel to mountain belts, *Phys. Earth planet. Inter.*, **78**, 337–342.
- Nicolas, A. & Christensen, N.I., 1987. Formation of anisotropy in upper-mantle peridotites—a review, in *Composition, Structure and Dynamics of the Lithosphere-Asthenosphere System*, eds Fuchs, K. & Froidevaux, C., *AGU Geodyn. Ser.*, **71**, 111–123.
- Nuttli, O., 1961. The effect of the earth's surface on the S-wave particle motion, *Bull. seism. Soc. Am.*, **51**, 237–246.
- Paech, H.J., Laiba, A.A., Shulyatin, N.D., Aleksashin, N.D. & Traube, V.V., 1991. Contribution to the geology of Western Dronning Maud Land: present knowledge, latest results and unsolved problems, *Zeitschrift geol. Wissenschaften*, **19**, 127–143.
- Ploverová, J., Šilený, J. & Babuška, V., 1996. Joint interpretation of upper-mantle anisotropy based on teleseismic P-travel time delays and inversion of shear-wave splitting parameters, *Phys. Earth planet. Inter.*, **95**, 293–310.
- Pondrelli, S. & Azzara, R., 1998. Upper mantle anisotropy in Victoria Land (Antarctica), *Pageoph.*, **151**, 433–442.
- Russo, R.M. & Silver, P.G., 1994. Trench-parallel flow beneath the Nazca Plate from seismic anisotropy, *Science*, **263**, 1105–1111.
- Russo, R.M., Silver, P.G., Franke, M., Ambeh, W.B. & James, D.E., 1996. Shear-wave splitting in northeast Venezuela, Trinidad, and the eastern Caribbean, *Phys. Earth planet. Inter.*, **95**, 251–275.
- Savage, M.K., 1999. Seismic anisotropy and mantle deformation: what have we learned from shear wave splitting?, *Rev. Geophys.*, **37**, 65–106.
- Schöne, T. & Schenke, H.-W., 1997. The gravity field of the southern Weddell Sea from GEOSAT and ERS-1, in *The Antarctic Region: Geological Evolution and Processes*, *Terra Antarctica*, pp. 1123–1128, ed. Ricci, C.A., Siena.
- Silver, P.G., 1996. Seismic anisotropy beneath the continents: probing the depth of geology, *Ann. Rev. Earth planet. Sci.*, **24**, 385–432.
- Silver, P.G. & Chan, W.W., 1991. Shear-wave splitting and subcontinental mantle deformation, *J. geophys. Res.*, **96**, 16 429–16 454.
- Silver, P.G. & Savage, M.K., 1994. The interpretation of shear-wave splitting in the presence of two anisotropic layers, *Geophys. J. Int.*, **119**, 949–963.
- Środa, P., Grad, M. & Guterch, A., 1997. Seismic models of the Earth's crustal structure between the South Pacific and the Antarctic Peninsula, in *The Antarctic Region: Geological Evolution and Processes*, *Proc. VII Int. Symp. on Antarctic Earth Sciences*, Siena, pp. 685–689, ed. Ricci, C.A., Terra Antarctica Publication, Siena.
- Steinhage, D., Nixdorf, U., Meyer, U. & Miller, H., 1999. New maps of the ice thickness and subglacial topography in Dronning Maud Land, Antarctica, determined by means of airborne radio echo sounding, *Ann. Glaciol.*, **29**, 267–272.

- Storey, B.C., Pankhurst, R.J. & Johnson, A.C., 1994. The Grenville Province within Antarctica: a test for the SWEAT hypothesis, *J. geol. Soc. Lond.*, **151**, 1–4.
- Storey, B.C., Vaughan, A.P.M. & Millar, I.L., 1996. Geodynamic evolution of the Antarctic Peninsula during Mesozoic times and its bearing on the Weddell Sea history, the continental margin off East Antarctica between 10°W and 30°W, in *Weddell Sea Tectonics and Gondwana Break-up*, eds Storey, B.C., King, E.C. & Livermore, R.A., *Geol. Soc. Lond. Spec. Publ.*, **108**, 87–104.
- Vachez, A., Barruol, G. & Tommasi, A., 1997. Why do continents break up parallel to ancient orogenic belts?, *Terra Nova*, **9**, 62–66.
- Vachez, A., Tommasi, A., Barruol, G. & Maumus, J., 2000. Upper mantle deformation and seismic anisotropy in continental rifts, *Phys. Chem. Earth (A)*, **25**, 111–117.
- Veit, A. & Miller, H., 1999. Mantle flow, plate motion and their influence in the geochemical evolution of Antarctic Peninsula Pliocene to recent volcanic rocks, *8th Int. Symp. on Antarctic Earth Sciences—Programme & Abstracts*, p. 310, Wellington, New Zealand.
- Vinnik, L.P., Kind, R., Kosarev, G.L. & Makayeva, L.I., 1989. Azimuthal anisotropy in the lithosphere from observations of long period *S* waves, *Geophys. J. Int.*, **99**, 549–559.
- Vinnik, L.P., Makayeva, L.I., Milev, A. & Usenko, Yu.A., 1992. Global patterns of azimuthal anisotropy and deformations in the continental mantle, *Geophys. J. Int.*, **111**, 433–447.
- Wessel, P. & Smith, W.H.F., 1998. New, improved version of Generic Mapping Tools released, *EOS, Trans. Am. geophys. Un.*, **79**, 579.
- White, R. & McKenzie, D., 1989. Magmatism at rift zones. The generation of volcanic continental margins and flood basalts, *J. geophys. Res.*, **94**(B6), 7685–7729.
- Wolfe, C.J. & Silver, P.G., 1998. Seismic anisotropy of oceanic upper mantle: shear-wave splitting methodologies and observations, *J. geophys. Res.*, **103**, 749–771.
- Xie, J., 1992. Shear-wave splitting near Guam, *Phys. Earth planet. Inter.*, **72**, 211–219.
- Yang, X., Fischer, K.M. & Abers, G.A., 1995. Seismic anisotropy beneath the Shumagin Islands segment of the Aleutian-Alaska subduction zone, *J. geophys. Res.*, **100**, 18 165–18 178.